

Discovery and Structure–Activity Relationship of 3-Methoxy-*N*-(3-(1-methyl-1*H*-pyrazol-5-yl)-4-(2-morpholinoethoxy)phenyl)benzamide (APD791): A Highly Selective 5-Hydroxytryptamine_{2A} Receptor Inverse Agonist for the Treatment of Arterial Thrombosis

Yifeng Xiong,* Bradley R. Teegarden, Jin-Sun Karoline Choi, Sonja Strah-Pleynet, Marc Decaire, Honnappa Jayakumar, Peter I. Dosa, Martin D. Casper, Lan Pham, Konrad Feichtinger, Brett Ullman, John Adams, Diane Yuskis, John Frazer, Michael Morgan, Abu Sadeque, Weichao Chen, Robert R. Webb, Daniel T. Connolly, Graeme Semple, and Hussien Al-Shamma

Arena Pharmaceuticals, 6166 Nancy Ridge Drive, San Diego, California 92121

Received January 13, 2010

Serotonin, which is stored in platelets and is released during thrombosis, activates platelets via the 5-HT_{2A} receptor. 5-HT_{2A} receptor inverse agonists thus represent a potential new class of antithrombotic agents. Our medicinal program began with known compounds that displayed binding affinity for the recombinant 5-HT_{2A} receptor, but which had poor activity when tested in human plasma platelet inhibition assays. We herein describe a series of phenyl pyrazole inverse agonists optimized for selectivity, aqueous solubility, antiplatelet activity, low hERG activity, and good pharmacokinetic properties, resulting in the discovery of **10k** (APD791). **10k** inhibited serotonin-amplified human platelet aggregation with an IC₅₀ = 8.7 nM and had negligible binding affinity for the closely related 5-HT_{2B} and 5-HT_{2C} receptors. **10k** was orally bioavailable in rats, dogs, and monkeys and had an acceptable safety profile. As a result, **10k** was selected for further evaluation and advanced into clinical development as a potential treatment for arterial thrombosis.

Introduction

Arterial thrombosis is the formation of a blood clot or thrombus inside an artery or arteriole that restricts or blocks the flow of blood and, depending upon location, can result in acute coronary syndrome or stroke. The formation of a thrombus is usually initiated by blood vessel injury, which triggers platelet aggregation and adhesion of platelets to the vessel wall. Treatments aimed at inhibiting platelet aggregation have demonstrated clear clinical benefits in the setting of acute coronary syndrome and stroke. Current antiplatelet therapies include aspirin, which irreversibly inhibits cyclooxygenase (COX^a) and results in reduced thromboxane production, clopidogrel and prasugrel, which inhibit platelet adenosine diphosphate (ADP) P₂Y₁₂ receptors, and platelet glycoprotein IIb/IIIa receptor antagonists. Another class of antiplatelet drugs, protease-activated thrombin receptor (PAR-1) antagonists, are also being evaluated in the clinic for the treatment of acute coronary syndrome.^{1a} The most advanced candidate in this class, *N*-[(1*R*,3*aR*,4*aR*,6*R*,8*aR*,9*S*,9*aS*)-9-{2-[5-(3-fluorophenyl)pyridin-2-yl]vinyl}-1-methyl-3-oxoperhydro-naphtho[2,3-*c*]furan-6-yl]-carbamic acid ethyl ester (SCH-530348), is currently in phase 3 trials for the prevention of arterial thrombosis.^{1b,c}

The 5-HT_{2A} receptor is one of 15 different serotonin receptor subtypes.² In the cardiovascular system, modulation of 5-HT_{2A} receptors on vascular smooth muscle cells and platelets is thought to play an important role in the regulation of cardiovascular function.^{3,4} Platelets are activated by a variety of agonists such as ADP, thrombin, thromboxane, serotonin, epinephrine, and collagen. Upon platelet activation at the site of blood vessel injury, a number of factors including serotonin (5-HT) are released. Although by itself serotonin is a weak activator of platelet aggregation, in vitro it can amplify aggregation induced by other agonists as mentioned above.^{5,6} Therefore, serotonin released from activated platelets may induce further platelet aggregation and enhance thrombosis.

The 5-HT_{2A} receptor antagonist ketanserin (Figure 1) was shown in clinical studies to reduce early restenosis⁷ and decrease myocardial ischemia during coronary balloon angioplasty.⁸ However, in another study, ketanserin did not significantly improve clinical outcomes, and the rate of adverse events was higher than that observed in the control group.⁹ Some of the adverse events reported in the latter study could be specific to ketanserin and resulted from its lack of 5-HT_{2A} receptor selectivity. Other 5-HT_{2A} antagonists with improved selectivity profiles have shown promise in clinical studies. For example, sarpgrelate (Figure 1) was shown to inhibit restenosis following coronary stenting.¹⁰

Because the 5-HT_{2A} receptor is expressed both in peripheral tissues and in the central nervous system (CNS), compounds with limited CNS partitioning would be preferred to maximize cardiovascular and blood platelet pharmacological activity while minimizing CNS effects. In addition, because 5-HT_{2A}

*To whom correspondence should be addressed. Phone: +1 858-453-7200. Fax: +1 858-453-7210. E-mail: yxiong@arenapharm.com.

^a Abbreviations: COX, cyclooxygenase; ADP, adenosine diphosphate; SAR, structure–activity relationship; hERG, human ether-a-go-go-related gene; CNS, central nervous system; 5-HT, serotonin; AUC, area under the plasma concentration time curve, iv, intravenous; IP, inositol phosphate.

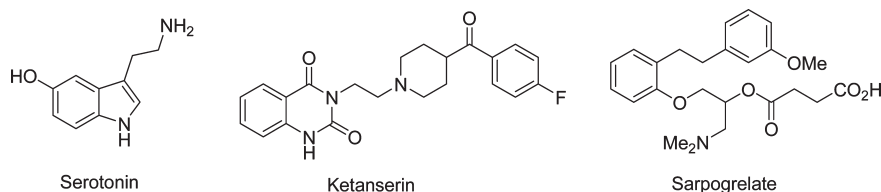


Figure 1. Serotonin and known 5-HT_{2A} receptor antagonists.

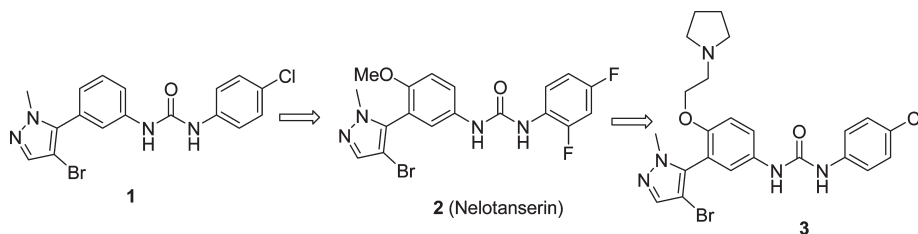
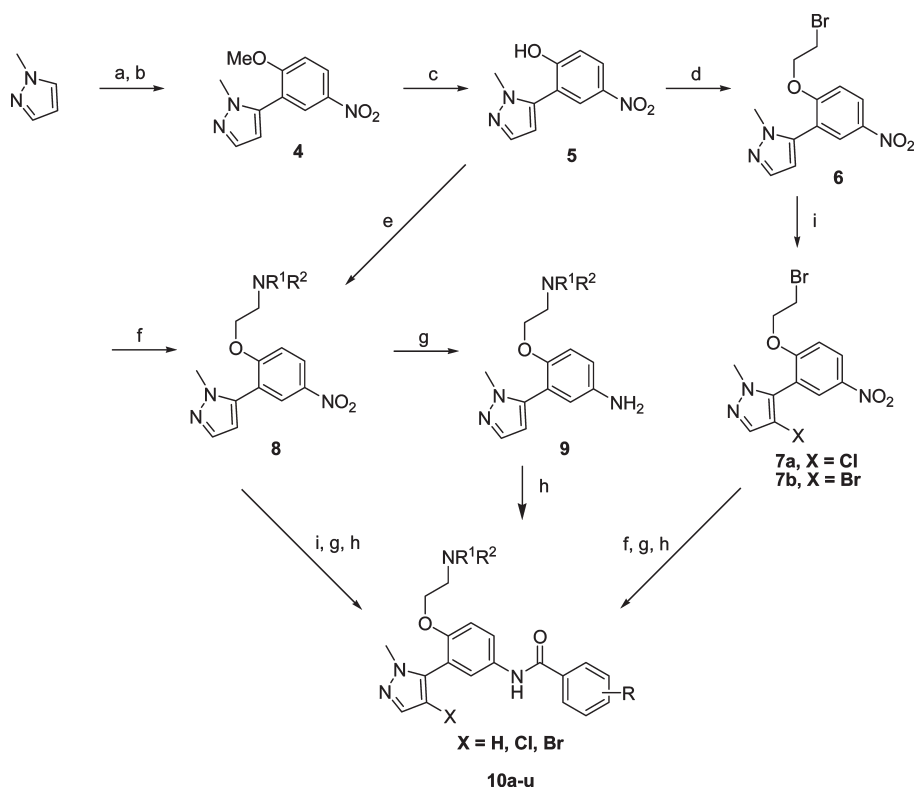


Figure 2. Phenyl-pyrazole urea based 5-HT_{2A} receptor inverse agonists.

Scheme 1. Synthesis of Phenyl-Pyrazole Amide Derivatives^a



^a Reagents and conditions: (a) *n*-BuLi, THF at -78 °C, then ZnCl₂; (b) 2-iodo-4-nitroanisole, Pd(PPh₃)₄; (c) AlCl₃, 1,2-dichloroethane; (d) 1,2-dibromoethane, K₂CO₃, DMSO; (e) HOCH₂CH₂NR¹R², Ph₃P, DIAD, THF; (f) HNR¹R², K₂CO₃, DMF; (g) zinc dust, NH₄Cl, THF; (h) R-PhCO₂H, HATU, triethylamine, DMF or R-Ph-COCl, triethylamine, THF; (i) NBS or NCS, MeOH or DMF.

receptor inverse agonists are thought to reduce thrombus formation via inhibition of serotonin-mediated amplification of platelet aggregation without inhibiting agonist driven aggregation per se, it is possible that this class of inhibitors will have an improved bleeding risk side effect profile compared to what has been observed with other classes of antithrombotic drugs.

We have previously identified a series of phenyl-pyrazole urea-based 5-HT_{2A} inverse agonists (e.g., compound 1, Figure 2).¹¹ This structure–activity relationship (SAR) effort led to the discovery of 2 (Nelotanserin, Figure 2), which was advanced into clinical trials for the treatment of insomnia.¹²

Although such ureas are potent 5-HT_{2A} inverse agonists, they were found to possess limited aqueous solubility, a property that we thought would be important for good antiplatelet activity. We have since reported on modifications to this urea series in which we incorporated amino moieties into the scaffold. The resulting series of phenyl-pyrazole ureas as exemplified by 3^{13–15} were significantly more soluble in aqueous solution. Moreover these compounds also showed improved inhibition of platelet aggregation.¹⁴ Unfortunately, many of these solubilized ureas had suboptimal selectivity profiles and poor pharmacokinetic properties. To further explore the scope of the soluble phenyl-pyrazole scaffold, with a particular goal

of improving the pharmacokinetic and pharmaceutical characteristics, the SAR was expanded from ureas to sulfonamides, carbamates, and amides. Herein, we describe SAR efforts that led to the identification of **10k** (APD791), a highly selective 5-HT_{2A} inverse agonist with high receptor binding affinity, potent activity on human platelets, a clean safety profile, and outstanding pharmaceutical properties.

Chemistry

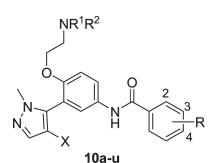
The syntheses of the 1-*N*-alkyl-5-phenyl-pyrazole scaffold **4**, its subsequent modification to introduce a basic amine moiety to provide intermediates **8**, and formation of final amides **10** are outlined in Scheme 1. Starting with commercially available *N*-methyl pyrazole, lithiation with *n*-BuLi followed by a Negishi coupling with 2-iodo-4-nitroanisole furnished intermediate **4**.¹³ Demethylation with aluminum trichloride afforded phenol **5**. Reaction with 1,2-dibromoethane gave the bromo-tethered compound **6**. Alkylation of **6** with a series of amines introduced basic functionalities into the molecules providing **8**. Alternatively, **8** could also be prepared via Mitsunobu reaction from phenol **5** and the appropriate amino-ethanol derivatives. Reduction of the nitro group with zinc dust afforded anilines **9**, which were then coupled with acids or acid chlorides to furnish the desired amides **10**.¹³ Halogenation of the pyrazole ring, where appropriate, could be effected at different stages. Bromo-tethered analogue **6** was treated with either *N*-chlorosuccinimide (NCS) or *N*-bromosuccinimide (NBS) to form chloro or bromo pyrazoles **7a** and **7b**, respectively. Amination, reduction, and amidation of **7** led to the final products **10**. Alternatively, halogens could be introduced after the amine moiety was incorporated from **8**, and thus halogenation, subsequent reduction, and amidation of **8** provided an alternative approach to final products **10**.

Results and Discussion

In vitro competitive binding assays with radiolabeled 2,5-dimethoxy-4-iodoamphetamine (¹²⁵I-DOI) were used to determine *K*_i values for all compounds against recombinant h5-HT_{2A} and h5-HT_{2C} receptors (Table 1). Compounds were also tested for inhibition of serotonin-induced amplification of ADP-stimulated platelet aggregation in human platelet rich plasma, and in selected cases, for human ether-a-go-go-related gene (hERG) inhibition in a patch clamp assay (Table 1). As previously observed in the phenyl-pyrazole urea series, the phenyl-pyrazole amides showed excellent affinity for the 5-HT_{2A} receptor. In addition, and in contrast to the urea series,¹⁴ the amides generally showed a very high degree of selectivity for the 5-HT_{2A} receptor over the 5-HT_{2C} receptor. In all the examples tested, the selectivity over the 5-HT_{2B} receptor was uniformly high and thus affinity for this receptor was not examined on a routine basis.

A wide range of monosubstitutions on the phenyl ring was evaluated, all well tolerated regardless of the electron withdrawing or donating groups. The *meta*-substituted analogues were found to be higher affinity ligands for the 5-HT_{2A} receptor than the *para*-substituted analogues. For example, the *meta*-F analogue **10e** and *meta*-CF₃ analogue **10i** had slightly higher affinity than the corresponding *para*-F analogue **10f** and *para*-CF₃ analogue **10h**. Furthermore, the *meta*-substituted analogues were more selective for the 5-HT_{2A} receptor than the *para*-substituted analogues. For instance, **10b** (*meta*-CF₃) had lower affinity at the 5-HT_{2C} receptor and slightly higher affinity at the 5-HT_{2A} receptor than **10a** (*para*-CF₃),

Table 1. Binding Affinities of Compounds **10a–u** at Human 5-HT_{2A} and 5-HT_{2C} Receptors, Activity of Inhibition of Serotonin Mediated Amplification of ADP-Stimulated Human Platelet Aggregation and Inhibition of hERG Channel



Comp.	NR ¹ R ²	X	R	5-HT _{2A} <i>K</i> _i ^a (nM)	5-HT _{2C} <i>K</i> _i ^a (nM)	Inhibition of Platelet Aggregation IC ₅₀ (nM) (n)	hERG ^b (% Inh.) (3 μM)
10a		H	4-CF ₃	1.9	225	2.0 (3)	66 ^c
10b		H	3-CF ₃	0.6	1140	3.2 (1)	80 ^c
10c		H	3-CF ₃	12	9250	189 (1)	50
10d		H	2,4-di-F	8.6	>10000	27 (4)	16 ^{c,e}
10e		H	3-F	5.1	>10000	86 (4)	43
10f		H	4-F	18	>10000	100 (1)	<i>d</i>
10g		Cl	3-F	0.6	3380	22 (2)	46
10h		H	4-CF ₃	2.4	5900	61 (8)	33 ^c
10i		H	3-CF ₃	0.7	>10000	18 (6)	50 ^{c,f}
10j		H	3,4-di-F	4.1	>10000	29 (3)	56
10k		H	3-OMe	4.9	>10000	8.7 (3)	32 ^g
10l		H	3-CF ₃	287	>10000	<i>d</i>	<i>d</i>
10m		Cl	3-CF ₃	5.3	>10000	127 (1)	53
10n		H	3-CF ₃	4.3	5614	145 (1)	75
10o		H	3-F	15	>10000	40 (5)	41 ^h
10p		Cl	3-F	2.2	8600	70 (1)	43
10q		H	3-OMe	4.5	>10000	77 (5)	24
10r		H	3-OMe	5.1	5890	57 (1)	17
10s		H	3-OMe	28	>10000	<i>d</i>	23
10t	NHCH ₂ CH ₂ OH	H	3-OMe	1.8	5874	5.8 (3)	36
10u	NH ₂	H	3-OMe	2.2	2347	6.9 (3)	22

^a *K*_i values are the mean of at least three experiments performed in triplicate, determined from 10 concentrations, all *K*_i values were calculated from IC₅₀ values using the method of Cheng and Prusoff²² with standard deviation < 0.4 log units. ^b hERG patch clamp assays were performed at Aviva Biosciences, San Diego, CA (<http://www.avivabio.com>). ^c Measured at 1 μM concentration. ^d Not determined. ^e IC₅₀ = 4.1 μM. ^f IC₅₀ = 0.9 μM. ^g IC₅₀ = 11 μM. ^h IC₅₀ = 4.1 μM.

making **10b** much more selective at the 5-HT_{2A} receptor (1900-fold) than **10a** (118-fold). Therefore, during lead optimization at other positions in the molecules (pyrazole halogenations and incorporation of amino functionalities), we focused more heavily on the *meta*- than *para*-substituted analogues. Among the different *meta*-substituents, lipophilic

CF₃ groups significantly enhanced the 5-HT_{2A} receptor affinity. For example, **10i** (*meta*-CF₃) had 6- to 7-fold higher affinity than **10k** (*meta*-OMe) or **10e** (*meta*-F) analogues.

The effect of pyrazole halogenation on receptor affinity was also examined. In general, bromination or chlorination of the pyrazole ring led to increased affinity for the 5-HT_{2A} receptor when compared directly to the nonhalogenated pyrazoles. For example, chlorination of **10l** provided **10m**, which showed a more than 50-fold increase in the 5-HT_{2A} receptor affinity. In another example, addition of a chlorine to **10e** resulted in **10g**, which showed a 8-fold improvement in 5-HT_{2A} receptor affinity.

A wide range of amino substituents was also evaluated. As shown in Table 1, almost all amino groups provided compounds with good binding affinity at the 5-HT_{2A} receptor with the exception of the oxo-piperazinyl group (**10l**), which was 20- to 480-fold weaker compared to other amino groups with the same phenyl ring and pyrazole ring substitutions. As discussed earlier, binding affinity with this amino group was improved by introducing a chlorine atom onto the pyrazole (**10m**). Whereas all amino groups showed good (e.g., 118-fold, **10a**) to excellent (e.g., 2040-fold, **10k**) selectivity for the 5-HT_{2A} receptor vs the 5-HT_{2C} receptor, a morpholino group appeared to be most beneficial, showing very little affinity for the 5-HT_{2C} receptor even with halogen substitutions on the pyrazole.

On the basis of their structural similarity to our previous series of 5-HT_{2A} receptor ligands (including **2**), which were all functional inverse agonists,¹² we expected the compounds in these current series to have the same functional response in vitro. In this current investigation, we confirmed this expectation for selected compounds using inhibition of total inositol phosphate (IP) accumulation as a functional assay to determine the inverse agonist potency.¹⁹ For example, **10b** had an IC₅₀ of 23 nM in the IP assay, and **10k** inhibited IP accumulation with an IC₅₀ of 5.2 nM.

After this initial examination of their receptor binding affinities and selectivity profile, compounds were then evaluated in a second functional (antagonist) assay for their ability to inhibit serotonin-mediated amplification of ADP-stimulated human platelet aggregation. As shown in Table 1, IC₅₀ values for inhibition of platelet aggregation ranged from 2 to 189 nM. In general, platelet activity did not correlate well with binding affinity, but compounds were usually somewhat less potent in the platelet inhibition assay than in the binding assay. The degree of difference between the K_i value in binding and the IC₅₀ value in the platelet assay varied from 1- to 2-fold (**10a** and **10k**) to 30-fold (**10n**) and depended on compound structure. Interestingly, removal of serum proteins from platelet rich plasma resulted in a left shift in the IC₅₀ for inhibition of platelet aggregation, suggesting that protein binding may play a significant role in the observed differences between platelet aggregation activity and receptor affinity. Hence, the platelet assay served as a useful guide to receptor activity in the presence of serum proteins, and only compounds with a modest shift between the values for the two assays were considered for further evaluation.

In general, compounds containing pyrrolidino and morpholino moieties had smaller shifts compared to compounds containing other basic amines. For example, **10j** and **10k** had same receptor affinity as **10m** and **10n**, but **10j** and **10k**, which had a morpholino moiety, are much more potent than **10m** or **10n** in the platelet assay. Halogen substitutions of the pyrazole usually increased binding affinities but not necessarily platelet

activities, as exemplified by **10p** and **10o**. Although, in another example, pyrazole chlorination was more successful, **10g** (chloro-pyrazole) being superior to **10e** in binding affinity as well as platelet activity. We reasoned that as compounds became more lipophilic after introduction of a halogen, they would likely be more protein bound, which in turn would result in a significantly greater shift between K_i in the binding assay and IC₅₀ values in the platelet assay. In contrast, we could discern no clear trend on how the substitutions on the phenyl ring affected the platelet activity.

After introducing basic amines into the scaffold, both aqueous solubility and platelet activity were improved, but one of the liabilities we observed was the introduction of a significant interaction with the hERG channel. As a result, compounds of interest were screened in a patch clamp electrophysiology assay at a single concentration of 3 or 1 μM (Table 1).

Several previously well-explored approaches were employed to attenuate hERG activity.^{16,17} The first was to reduce the pK_a of the basic nitrogen, which proved to be quite effective in reducing hERG activity while still maintaining the receptor affinity and platelet activity. As discussed earlier, both morpholino- and pyrrolidino-containing compounds trended toward improved potency in the platelet aggregation assay. However, due to the high pK_a of the pyrrolidine nitrogen, many of the pyrrolidino-containing compounds had very high activity in the hERG channel assay and were therefore dropped from further evaluation. In contrast, compounds with a morpholino-substituent had somewhat reduced activity at the hERG channel. For example, **10b** containing a pyrrolidine (pK_a 9.56)¹⁸ showed 80% inhibition at 1 μM while the analogous **10i**, which incorporated a morpholino-substituent (pK_a 6.38), showed only 50% inhibition at the same concentration. The pK_a of the basic nitrogen could also be reduced by introducing electron withdrawing groups adjacent to the amine moiety, again resulting in reduced hERG channel blockade. Compound **10c**, which contained a *gem*-difluoro-pyrrolidine (pK_a 4.91), had a further attenuation of hERG activity to 50% inhibition at 3 μM. Increasing the polarity of molecules (lowering clogP) is another well explored method of decreasing hERG activity. Compounds **10q**, **10r**, and **10s** all contained polar groups attached to the amine moiety and each had significantly lower hERG inhibition, typically less than 30% at 3 μM. In addition, **10q** (*meta*-OMe on phenyl ring, 24% inhibition at 3 μM) had lower hERG activity than **10n** (*meta*-CF₃ on phenyl ring, 75% inhibition at 3 μM), showing that making changes to other areas of the molecule to reduce clogP (in this case from 3.16 to 2.22) was also able to assist in decreasing hERG activity. This strategy of optimization of receptor affinity and selectivity and the subsequent management of platelet activity and hERG activity led us to the initial identification of our lead compound. **10k** was a selective, high affinity 5-HT_{2A} receptor inverse agonist with excellent activity in the platelet aggregation assay. In addition, **10k** showed only moderate hERG inhibition of 32% at 3 μM in the screening assay, and this translated into an IC₅₀ of 11 μM when tested in the same patch clamp assay in full concentration–response mode.

Another challenge encountered after introducing the basic amine functionality was the poor microsomal stability of compounds in rodents, which resulted in poor in vivo rodent pharmacokinetic parameters. Pharmacokinetic profiles of selected compounds in rat are shown in Table 2. In general, as expected with poor microsomal stability, most compounds

Table 2. Rat Pharmacokinetic Parameters of Selected Compounds after 10 mg/kg Oral Dose^a

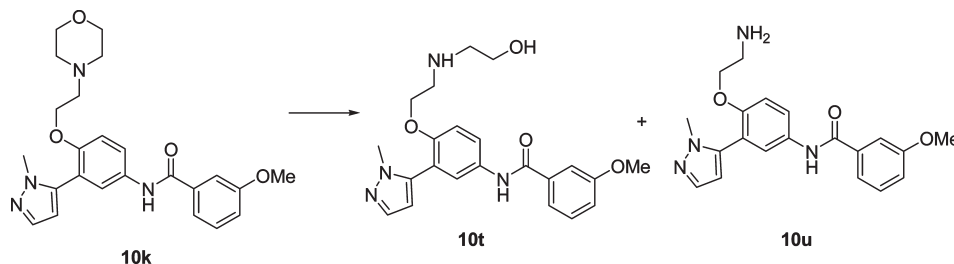
compd	C_{\max} (ng/mL)	AUC _{last} (h·ng/mL)	$T_{1/2}$ (h)	IV CL _{total} (L/h/kg)	V _{ss} (L/kg)	F (%) ^b
10d	56	171	1.5	14	11.7	22
10i	202	288	1.8	9.6	5.1	27
10a	453	3831	2.8	1.1	5.4	43

^a Values represent the mean of $n = 3$ animals. ^b % F calculated relative to a 2 mg/kg iv dosing.

Table 3. Pharmacokinetic Profile of **10k** in Preclinical Species after 10 mg/kg Oral Dose^a

species	C_{\max} (ng/mL)	AUC _{last} (h·ng/mL)	$T_{1/2}$ (h)	IV CL _{total} (L/h/kg)	V _{ss} (L/kg)	F (%) ^b
rat	58	43	1.0	22	29	10
dog	2280	3544	0.9	1.2	1.3	45
monkey	1462	1922	2.1	0.9	0.6	16

^a Values represent the mean of $n = 3$ animals. ^b % F calculated relative to a 2 mg/kg i.v. dosing.

**Figure 3.** Compound **10k** and its active metabolites **10t** and **10u**.

tested exhibited very high plasma clearance, low exposure, and poor oral bioavailability. Compound **10d** was a typical example (Table 2). We observed that a lipophilic CF₃ group sometimes improved these pharmacokinetic parameters. For example, **10i**, with a CF₃ group on the phenyl ring, had slightly lower clearance than **10g** and improved C_{\max} and AUC compared to **10d**. However, the hERG activity of **10i** prevented this compound from moving forward. The combination of a CF₃ group on the phenyl ring and a pyrrolidino group (**10a**) resulted in much lower clearance, very good exposure, and oral bioavailability. However, due to the high hERG activity and the significant 5-HT_{2C} receptor affinity, **10a** was not suitable for further development despite its potent platelet activity and good pharmacokinetic profile.

The pharmacokinetic profile of **10k** in preclinical species was initially somewhat unpromising (Table 3). Compound **10k** had modest pharmacokinetic characteristics in rats, but in monkeys and dogs, **10k** had quite acceptable pharmacokinetic properties. Plasma clearance was low, oral bioavailability was moderate to good, and overall exposure was high. In addition, two major active metabolites of **10k** were identified (Figure 3). **10t** and **10u** were generated upon incubation of **10k** with human, dog and rat liver microsomes and were also observed in vivo across all species tested. These two metabolites were essentially equipotent with **10k** in receptor affinity, inhibition of platelet aggregation, and target selectivity (Table 1). Remarkably, after lengthy struggles to control hERG inhibition within the series, the metabolites of **10k** also turned out to be only weak inhibitors of the hERG channel. Thus, there were no known off-target effects of these major metabolites that would preclude the further development of **10k**, and indeed, it was envisioned that their generation in vivo could extend the duration of biological activity for **10k**. Neither metabolite was suitable as a development candidate in its own right, however, as neither showed good exposure after oral administration, which we ascribed to lack of intestinal absorption.

The in vivo activity of **10k** was tested in beagle dogs using inhibition of ex vivo serotonin induced platelet aggregation and inhibition of arterial thrombosis in the Folts model, a classic canine model of recurrent coronary thrombosis, considered to mimic many of the key pathophysiologic features of unstable angina, as previously described.^{19,20} Levels of serotonin-mediated amplification of collagen-stimulated platelet aggregation were determined in whole blood following a single oral dose of 10 mg/kg of **10k**. Complete inhibition of serotonin-mediated aggregation was observed 1 h after dosing of **10k** and was maintained at the 6, 12, and 24 h time points with 86%, 57%, and 58% inhibition, respectively. Similar results were obtained using the ex vivo assay following 10 days of repeat dosing of **10k** at a 1 mg/kg dose.¹⁹ In the Folts model, **10k** attenuated recurrent thrombosis in anesthetized dogs either pretreated with **10k** or treated with **10k** after the onset of recurrent thrombosis, at a dose of 0.07 mg/kg iv bolus followed by continuous iv fusion of 1.16 μ g/kg/min. Flow-time area averaged 58–59% following administration of **10k** vs 21–28% in saline controls.²⁰ Overall, this profile, including the potential for an extended duration of action via the generation of active metabolites, was deemed sufficiently attractive for us to select **10k** for further development.

Summary

10k is a novel 5-HT_{2A} inverse agonist with high receptor binding affinity ($K_i = 4.9$ nM) and functional inverse agonism of inositol phosphate accumulation ($IC_{50} = 5.2$ nM).¹⁹ **10k** had excellent selectivity for the 5-HT_{2A} receptor versus 5-HT_{2C} ($K_i > 10000$ nM) and 5-HT_{2B} ($K_i > 10000$ nM) receptors in competition binding assays (> 2000-fold selectivity on both receptors). **10k** had limited CNS partitioning, with a brain to plasma ratio of 0.05 (based on C_{\max} at 30 mg/kg dose) in rat. Further profiling against a panel of 70 human GPCRs, ion channels, and transporters (Cerep) showed that **10k** had no appreciable activities on any other receptors or transporters tested. Patch clamp analysis suggested that **10k** had

limited hERG channel inhibition potential, with an IC_{50} of 11 μ M. On the basis of CYP450 inhibition assays using human liver microsomes, **10k** appeared to have little potential for drug–drug interactions. **10k** exhibited potent inhibition of serotonin mediated amplification of ADP-stimulated human and dog platelet aggregation (IC_{50} = 8.7 and 23.1 nM, respectively). Oral administration of **10k** to beagle dogs resulted in acute (1 h) and subchronic (10 day) inhibition of serotonin mediated amplification of collagen-stimulated platelet aggregation in whole blood ex vivo. In the Folts model, **10k** improved coronary patency even after the onset of recurrent thrombosis. Taken together, these data suggest that **10k**, a high affinity, selective, orally bioavailable 5-HT_{2A} receptor inverse agonist, represents a promising compound for development as an antiplatelet agent.

Experimental Section

Chemistry. All reagents were commercially available and used without further purification unless stated otherwise. Microwave irradiations were performed using either a Smith Synthesizer or an Emrys Optimizer (Biotage). Column chromatography was carried out on prepacked silica gel columns using KP-Sil supplied by Biotage and on silica gel columns using Kieselgel 60, 0.063–0.200 mm (Merck). Proton nuclear magnetic resonance (¹H NMR) spectra were recorded on a Bruker Avance-400 equipped with a Quad Nucleus probe (QNP) or a Broad-band Inverse (BBI) probe and z-gradient. Chemical shifts (δ) are given in parts per million (ppm), with the residual solvent signal used as a reference. Coupling constants (J) are reported in Hz. NMR abbreviations are used as follows: s = singlet, d = doublet, t = triplet, q = quartet, m = multiplet, dd = doublet of doublets, dt = doublet of triplets, b = broad. Melting points were recorded on differential scanning calorimetry (DSC).

Analytical HPLC/MS was conducted on a PE Sciex API 150EX mass spectrometer with an electrospray source, using a Shimadzu Inc. LC-10A VP UV detector monitoring at 214 nm, Analyst 1.2 software, and either (a) a Gilson 215 autosampler and an Alltech Prevail C18 column (5 μ , 250 mm \times 4.6 mm), using a gradient of 5% v/v CH₃CN (containing 1% v/v TFA) in H₂O (containing 1% v/v TFA) (t = 0.0 min) gradient to 95% v/v CH₃CN in H₂O (t = 6.0 min), 3.5 mL/min, or (b) a PE 200 autosampler and a Supelco Discovery C18 column (5 μ , 50 mm \times 2.1 mm), using a gradient of 5% v/v CH₃CN (containing 1% v/v TFA) in H₂O (containing 1% v/v TFA) (t = 0.0 min) gradient to 95% v/v CH₃CN in H₂O (t = 5.0 min), 0.75 mL/min. Preparative HPLC was conducted on a Varian Prostar reverse phase HPLC using either (a) a Phenomenex Luna C18 column (10 μ , 250 mm \times 21.2 mm), 5% (v/v) CH₃CN (containing 0.1% v/v TFA) in H₂O (containing 0.1% v/v TFA) gradient to 95% CH₃CN, 20 mL/min, λ = 220 nm, or (b) a Phenomenex Luna C18 column (10 μ , 250 mm \times 50 mm), 5% (v/v) CH₃CN (containing 0.1% v/v TFA) in H₂O (containing 0.1% v/v TFA) gradient to 95% CH₃CN, 50 mL/min, λ = 220 nm. The purity of all tested compounds was \geq 95% (peak area % at 214 nm) using the analytical methods described above unless stated otherwise.

5-(2-Methoxy-5-nitro-phenyl)-1-methyl-1H-pyrazole (4). A solution of *N*-methylpyrazole (5.12 g, 62.4 mmol) in THF (100 mL) was cooled to -78°C and 2.5 M *n*-butyllithium in hexane (27.5 mL, 68.8 mmol) was added. After stirring for 30 min at the same temperature, 0.5 M zinc chloride in THF (107 mL, 53.5 mmol) and 1 M zinc chloride in diethyl ether (15.3 mL, 15.2 mmol) were added. The mixture was allowed to warm up to room temperature and 2-iodo-4-nitroanisole (17.4 g, 62.4 mmol) followed by tetrakis-(triphenylphosphine)palladium (3.6 g, 3.1 mmol) were added. The reaction mixture was heated to 60 $^{\circ}\text{C}$ overnight. Once the reaction was complete, the solvents were removed under reduced pressure and the residue partitioned between ethyl acetate and brine. The

combined organic phases were dried over MgSO₄, filtered, and partly concentrated until a solid started to precipitate. Hexane (approximately 3 volumes) was added and the resultant precipitate collected by filtration and washed with a cold 3:1 mixture of hexane/ethyl acetate to afford **4** (8.6 g, 59%) as a yellow solid. ¹H NMR (400 MHz, CDCl₃) δ : 3.74 (s, 3H), 3.96 (s, 3H), 6.31 (d, J = 1.6 Hz, 1H), 7.08 (d, J = 9.2 Hz, 1H), 7.56 (d, J = 2.0 Hz, 1H), 8.19 (d, J = 2.8 Hz, 1H), 8.34 (dd, J = 2.8, 9.2 Hz, 1H). LCMS m/z = 234.1 [M + H]⁺.

2-(2-Methyl-2H-pyrazol-3-yl)-4-nitro-phenol (5). A mixture of **4** (3 g, 12.9 mmol) in 1,2-dichloroethane (50 mL) was cooled to 0 $^{\circ}\text{C}$ with stirring. Aluminum trichloride (6.9 g, 51.6 mmol) was added. The resulting mixture was heated at 80 $^{\circ}\text{C}$ for 3.5 h. The crude mixture was diluted with ethyl acetate and the solid removed by filtration. The resultant filtrate was washed with a 10% solution of potassium tartrate and the solvent removed by evaporation. The residue was purified by HPLC to give **5** as a yellow solid (1.08 g, 38%). ¹H NMR (400 MHz, DMSO-*d*₆) δ : 3.74 (s, 3H), 6.38 (d, J = 1.6 Hz, 1H), 7.16 (d, J = 9.2 Hz, 1H), 7.48 (d, J = 2.0 Hz, 1H), 8.05 (d, J = 2.8 Hz, 1H), 8.24 (dd, J = 2.8, 9.2 Hz, 1H), 12.0 (s, 1H). LCMS m/z = 220.1 [M + H]⁺.

5-[2-(2-Bromo-ethoxy)-5-nitro-phenyl]-1-methyl-1H-pyrazole (6). To a suspension of **5** (1.042 g, 4.76 mmol) in THF (50 mL) at rt was added triphenylphosphine (2.138 g, 8.15 mmol) and 2-bromoethanol (0.580 mL, 8.21 mmol). Diisopropyl azodicarboxylate (DIAD) (1.58 mL, 7.81 mmol) was added dropwise to the stirring mixture. On completion of the addition, the reaction mixture was stirred at rt for a further 2 h and then concentrated to yield an oil which was purified by SiO₂ column chromatography (eluent: 40% ethyl acetate/60% hexanes) to afford **6** (1.40 g, 90%) as a white solid. ¹H NMR (400 MHz, DMSO-*d*₆) δ : 3.73 (s, 3H), 3.82–3.77 (m, 2H), 4.59–4.54 (m, 2H), 6.43 (d, J = 1.8 Hz, 1H), 7.42 (d, J = 9.2 Hz, 1H), 7.51 (d, J = 1.8 Hz, 1H), 8.12 (d, J = 2.9 Hz, 1H), 8.36 (dd, J = 9.2, 2.9 Hz, 1H). LCMS m/z = 326.1/328.1 [M + H]⁺.

5-[2-(2-Bromo-ethoxy)-5-nitro-phenyl]-4-chloro-1-methyl-1H-pyrazole (7a). A mixture of **6** (470 mg, 1.44 mmol) and *N*-chlorosuccinimide (192 mg, 1.44 mmol) in DMF (2 mL) was heated under microwave irradiation at 100 $^{\circ}\text{C}$ for 20 min. The mixture was quenched with water, extracted with ethyl acetate, and the combined extracts dried in vacuo to give **7a** as a yellow solid (462 mg, 89%) which was used in subsequent reactions without purification. ¹H NMR (400 MHz, CDCl₃) δ : 3.55–3.61 (m, 2H), 3.78 (s, 3H), 4.44 (t, J = 5.6 Hz, 2H), 7.13 (d, J = 9.1 Hz, 1H), 7.57 (s, 1H), 8.23 (s, 1H), 8.40 (dd, J = 2.8, 9.1 Hz, 1H). LCMS m/z = 360.1/362.1 [M + H]⁺.

4-Bromo-5-[2-(2-bromo-ethoxy)-5-nitro-phenyl]-1-methyl-1H-pyrazole (7b). A mixture of **6** (200 mg, 0.61 mmol) and *N*-bromosuccinimide (109 mg, 0.61 mmol) in DMF (2 mL) was heated under microwave irradiation at 100 $^{\circ}\text{C}$ for 10 min. The mixture was quenched with water, extracted with ethyl acetate, and the combined extracts dried in vacuo to give **7b** as a yellow solid (200 mg, 81%), which was used in subsequent reactions without purification. ¹H NMR (400 MHz, CDCl₃) δ : 3.53–3.64 (m, 2H), 3.78 (s, 3H), 4.38–4.49 (m, 2H), 7.11 (d, J = 9.1 Hz, 1H), 7.57 (s, 1H), 8.23 (s, 1H), 8.39 (dd, J = 2.8, 9.1 Hz, 1H). LCMS m/z = 404.1/406.1/407.9 [M + H]⁺.

General Procedure A, Preparation of Intermediates 8 via Alkylation: 1-Methyl-5-[5-nitro-2-[2-(pyrrolidin-1-yl)ethoxy]phenyl]-1H-pyrazole (8a). A mixture of **6** (390 mg, 1.20 mmol), pyrrolidine (104 mg, 1.46 mmol), and potassium carbonate (218 mg, 1.58 mmol) in DMF (4 mL) was heated under microwave irradiation at 100 $^{\circ}\text{C}$ for 15 min. The resulting mixture was purified by HPLC to give the TFA salt of **8a** as a yellow solid (400 mg, 77%). ¹H NMR (400 MHz, CD₃CN) δ : 1.80–1.88 (m, 2H), 1.94–2.00 (m, 2H), 2.79–2.89 (m, 2H), 3.37–3.45 (m, 2H), 3.48–3.53 (m, 2H), 3.72 (s, 3H), 4.43–4.46 (m, 2H), 6.40 (d, J = 2.0 Hz, 1H), 7.25 (d, J = 9.2 Hz, 1H), 7.56 (d, J = 2.0 Hz, 1H), 8.20 (d, J = 2.9 Hz, 1H), 8.38 (dd, J = 2.9, 9.2 Hz, 1H). LCMS m/z = 317.2 [M + H]⁺.

5-[2-[2-(3,3-Difluoropyrrolidin-1-yl)ethoxy]-5-nitrophenyl]-1-methyl-1H-pyrazole (8c). 8c was prepared in a manner similar to that described for 8a, using 6 (50 mg, 0.15 mmol) and 3,3-difluoropyrrolidine hydrochloride (26 mg, 0.18 mmol) as starting materials, to give the TFA salt of 8c as a yellow solid (16 mg, 22%). ¹H NMR (400 MHz, CD₃CN) δ: 2.35–2.45 (m, 2H), 3.31–3.43 (m, 4H), 3.49–3.56 (m, 2H), 3.69 (s, 3H), 4.46–4.49 (m, 2H), 6.34–6.36 (m, 1H), 7.22 (d, *J* = 9.3 Hz, 1H), 7.49–7.50 (m, 1H), 8.18 (d, *J* = 3.0 Hz, 1H), 8.38 (dd, *J* = 2.9, 9.0 Hz, 1H). LCMS *m/z* = 353.3 [M + H]⁺.

4-[2-[2-(2-Methyl-2H-pyrazol-3-yl)-4-nitro-phenoxy]-ethyl]-morpholine (8d). A mixture of triphenylphosphine (7.5 g, 28.6 mmol) and diisopropyl azodicarboxylate (5.66 mL, 28.6 mmol) in THF (50 mL) was stirred at 0 °C for 10 min, then 5 (3.5 g, 15.9 mmol) and 2-morpholin-4-yl-ethanol (3.66 mL, 28.6 mmol) were added at 0 °C. The reaction mixture was allowed to warm to rt and was stirred for another hour. The solvent was removed in vacuo, and the crude mixture was purified by HPLC to provide 8g as a yellow solid (9.44 g, 89%). ¹H NMR (400 MHz, DMSO-*d*₆) δ: 2.92–3.58 (m, 6H), 3.69 (s, 3H), 3.75–3.85 (m, 2H), 4.54–4.56 (m, 2H), 4.77–4.85 (m, 2H), 6.39 (d, *J* = 1.8 Hz, 1H), 7.45 (d, *J* = 9.2 Hz, 1H), 7.52 (d, *J* = 1.8 Hz, 1H), 8.16 (d, *J* = 2.9 Hz, 1H), 8.43 (dd, *J* = 9.2, 2.9 Hz, 1H), 8.88 (s, 1H). LCMS *m/z* = 333.4 [M + H]⁺.

4-[2-[2-(1-Methyl-1H-pyrazol-5-yl)-4-nitrophenoxy]ethyl]-piperazin-2-one (8l). 8l was prepared in a manner similar to that described for 8a, using 6 (500 mg, 1.53 mmol) and piperazin-2-one (153 mg, 1.53 mmol) as starting materials. The TFA salt of 8l was isolated as a yellow solid (353 mg, 67%). ¹H NMR (400 MHz, DMSO-*d*₆) δ: 2.07 (s, 2H), 3.11–3.23 (m, 4H), 3.42–3.52 (m, 2H), 3.60–3.66 (m, 1H), 3.69 (s, 3H), 4.51–4.56 (m, 2H), 6.40 (d, *J* = 1.9 Hz, 1H), 7.45 (d, *J* = 9.3 Hz, 1H), 7.52 (d, *J* = 1.9 Hz, 1H), 8.16 (d, *J* = 2.9 Hz, 1H), 8.43 (dd, *J* = 9.2, 2.9 Hz, 1H). LCMS *m/z* = 346.1 [M + H]⁺.

1-[4-[2-(1-Methyl-1H-pyrazol-5-yl)-4-nitrophenoxy]ethyl]-piperazin-1-yl]ethanone (8n). 8n was prepared in a manner similar to that described for 8a, using 6 (325 mg, 1.0 mmol) and 1-(piperazin-1-yl)ethanone (153 mg, 1.2 mmol) as starting materials, to give the TFA salt of 8n as a yellow solid (423 mg, 100%). ¹H NMR (400 MHz, DMSO-*d*₆) δ: 2.02 (s, 3H), 2.74–3.40 (m, 6H), 3.50–3.60 (m, 2H), 3.68 (s, 3H), 3.75–4.35 (m, 2H), 4.50–4.60 (m, 2H), 6.40 (d, *J* = 1.9 Hz, 1H), 7.45 (d, *J* = 9.3 Hz, 1H), 7.54 (d, *J* = 1.9 Hz, 1H), 8.16 (d, *J* = 2.9 Hz, 1H), 8.43 (dd, *J* = 9.2, 2.9 Hz, 1H). LCMS *m/z* = 374.3 [M + H]⁺.

General Procedure B, Reduction of Nitro Group to Intermediates 9: 3-(1-Methyl-1H-pyrazol-5-yl)-4-[2-(pyrrolidin-1-yl)ethoxy]-aniline (9a). To a solution of 8a (2.52 g, 7.98 mmol) in saturated ammonium chloride (4 mL), water (4 mL), and THF (10 mL) was added zinc dust (2.81 g, 43 mmol) at 0 °C. The mixture was stirred at rt for 1 h and then filtered through a pad of celite to remove the solids. The filtrate was concentrated in vacuo to give 9a as a white solid in essentially quantitative yield (2.24 g). LCMS *m/z* = 287.2 [M + H]⁺. The product was used in the next step without purification.

4-[2-(3,3-Difluoropyrrolidin-1-yl)ethoxy]-3-(1-methyl-1H-pyrazol-5-yl)aniline (9c). 9c was prepared from 8c (258 mg, 0.73 mmol) in a manner similar to that described for 9a, providing 9c as a white solid in quantitative yield (230 mg). LCMS *m/z* = 323.2 [M + H]⁺. The product was used in the next step without further purification.

3-(1-Methyl-1H-pyrazol-5-yl)-4-(2-morpholinoethoxy)aniline (9d). 9d was prepared from 8d (1.91 g, 5.75 mmol) in a manner similar to that described for 9a, providing 9d as a white solid in quantitative yield (1.87 g). LCMS *m/z* = 303.4 [M + H]⁺. The product was used in the next step without further purification.

4-[2-[4-Amino-2-(1-methyl-1H-pyrazol-5-yl)phenoxy]ethyl]-piperazin-2-one (9l). 9l was prepared from 8l (353 mg, 1.02 mmol) in a manner similar to that described for 9a, providing 9l as a white solid (245 mg, 76%). LCMS *m/z* = 315.8 [M + H]⁺. The product was used in the next step without further purification.

1-[4-[2-(4-Amino-2-(1-methyl-1H-pyrazol-5-yl)phenoxy)ethyl]-piperazin-1-yl]ethanone (9n). 9n was prepared from 8n (373 mg, 0.67 mmol) in a manner similar to that described for 9a, providing 9n as a white solid (180 mg, 78%). LCMS *m/z* = 344.1 [M + H]⁺. The product was used in the next step without further purification.

General Procedure C, Preparation of Amides 10 via HATU Coupling: N-[3-(2-Methyl-2H-pyrazol-3-yl)-4-(2-pyrrolidin-1-yl-ethoxy)-phenyl]-4-trifluoromethyl-benzamide (10a). A mixture of 9a (57 mg, 0.2 mmol), 4-trifluoromethyl-benzoic acid (42 mg, 0.22 mmol), *N,N,N',N'*-tetramethyl-*O*-(7-azabenzotriazol-1-yl)-uronium hexafluorophosphate (HATU, 91 mg, 0.24 mmol) and triethylamine (0.1 mL) in DMF (2 mL) was heated under microwave irradiation at 100 °C for 15 min. After removal of excess solvent, the crude product was purified by HPLC to give the TFA salt of 10a as a white solid (65 mg, 71%). ¹H NMR (DMSO-*d*₆, 400 MHz) δ: 1.73–1.76 (m, 2H), 1.87–1.92 (m, 2H), 2.85–2.90 (m, 2H), 3.29–3.32 (m, 2H), 3.53–3.57 (m, 2H), 3.69 (s, 3H), 4.32 (t, *J* = 4.8 Hz, 2H), 6.32 (d, *J* = 2.0 Hz, 1H), 7.26 (d, *J* = 8.6 Hz, 1H), 7.50 (d, *J* = 1.8 Hz, 1H), 7.75 (d, *J* = 2.5 Hz, 1H), 7.88–7.94 (m, 3H), 8.15 (d, *J* = 8.8 Hz, 2H), 9.81 (s, 1H), 10.5 (s, 1H). LCMS *m/z* = 459.4 [M + H]⁺.

[3-(2-Methyl-2H-pyrazol-3-yl)-4-(2-pyrrolidin-1-yl-ethoxy)-phenyl]-3-trifluoromethyl-benzamide (10b). 10b was prepared in a manner similar to that described for 10a, using 9a (57 mg, 0.2 mmol) and 3-trifluoromethyl-benzoic acid (57 mg, 0.3 mmol) to give the TFA salt of 10b as a white solid (42 mg, 46%). ¹H NMR (CD₃CN, 400 MHz) δ: 1.25–1.40 (m, 2H), 1.81–1.88 (m, 2H), 2.79–2.82 (bs, 2H), 3.36–3.46 (m, 4H), 3.71 (s, 3H), 4.32 (t, *J* = 4.8 Hz, 2H), 6.29 (d, *J* = 1.9 Hz, 1H), 7.13 (d, *J* = 8.9 Hz, 1H), 7.46 (d, *J* = 1.9 Hz, 1H), 7.64 (d, *J* = 2.8 Hz, 1H), 7.72 (t, *J* = 7.8 Hz, 1H), 7.80 (dd, *J* = 2.9, 8.9 Hz, 1H), 7.89 (d, *J* = 7.9 Hz, 1H), 8.17 (d, *J* = 7.9 Hz, 1H), 8.23 (s, 1H), 8.95 (s, 1H). LCMS *m/z* = 459.4 [M + H]⁺.

General Procedure D, Preparation of Amides 10 via Acid Chloride Coupling: N-[4-[2-(3,3-Difluoropyrrolidin-1-yl)ethoxy]-3-(1-methyl-1H-pyrazol-5-yl)phenyl]-3-(trifluoromethyl)-benzamide (10c). A mixture of 9c (64 mg, 0.2 mmol), 3-trifluoromethylbenzoyl chloride (62 mg, 0.3 mmol), and triethylamine (0.1 mL) in THF (2 mL) was stirred at room temperature for 20 min. The solvent was evaporated and the crude product was purified by HPLC to give the TFA salt of 10c as a white solid (33 mg, 33%). ¹H NMR (acetone-*d*₆, 400 MHz) δ: 2.43–2.52 (m, 2H), 3.38–3.46 (m, 4H), 3.56–3.61 (m, 2H), 3.75 (s, 3H), 4.45 (t, *J* = 4.5 Hz, 2H), 6.29 (s, 1H), 7.22 (d, *J* = 8.8 Hz, 1H), 7.44 (s, 1H), 7.79–7.81 (m, 2H), 7.91–7.95 (m, 2H), 8.30 (d, *J* = 8.3 Hz, 2H), 9.82 (s, 1H). LCMS *m/z* = 495.3 [M + H]⁺.

2,4-Difluoro-N-[3-(2-Methyl-2H-pyrazol-3-yl)-4-(2-morpholin-4-yl-ethoxy)-phenyl]-benzamide. (10d). 10d was prepared in a manner similar to that described for 10c, using 9d (200 mg, 0.66 mmol) and 2,4-difluorobenzoyl chloride (140 mg, 0.79 mmol) to give the TFA salt of 10d as a white solid (99 mg, 34%); mp (HCl salt, recrystallized from iPrOH) 140–142 °C. ¹H NMR (acetone-*d*₆, 400 MHz) δ: 2.92–3.06 (m, 2H), 3.13–3.17 (m, 2H), 3.50–3.58 (m, 2H), 3.68 (s, 3H), 3.82–3.85 (m, 4H), 4.36 (t, 2H), 6.29 (s, 1H), 7.24 (d, *J* = 9.1 Hz, 2H), 7.44 (dt, *J* = 10.1, 2.8 Hz, 1H), 7.49 (s, 1H), 7.67 (s, 1H), 7.72–7.79 (m, 1H), 7.81 (dd, *J* = 9.1, 2.8 Hz, 1H), 9.43 (s, 1H). LCMS *m/z* = 443.5 [M + H]⁺.

3-Fluoro-N-[3-(2-methyl-2H-pyrazol-3-yl)-4-(2-morpholin-4-yl-ethoxy)-phenyl]-benzamide (10e). 10e was prepared in a manner similar to that described for 10c, using 9d (120 mg, 0.40 mmol) and 3-fluorobenzoyl chloride (76 mg, 0.47 mmol) to give the TFA salt of 10e as a white solid (102 mg, 61%). ¹H NMR (acetone-*d*₆, 400 MHz) δ: 2.99–3.25 (m, 2H), 3.25–3.49 (m, 2H), 3.69 (t, *J* = 4.5 Hz, 2H), 3.75 (s, 3H), 3.77–3.96 (m, 4H), 4.59 (t, *J* = 4.8 Hz, 2H), 6.30 (t, *J* = 1.5 Hz, 1H), 7.23 (d, *J* = 9.1 Hz, 1H), 7.36 (dt, *J* = 2.5, 8.6 Hz, 2H), 7.49 (t, *J* = 1.8 Hz, 1H), 7.54–7.61 (m, 1H), 7.74 (dt, *J* = 2.0, 9.8 Hz, 1H), 7.82 (t, *J* = 2.4 Hz, 1H), 7.84 (d, *J* = 7.8 Hz, 1H), 7.94 (dt, *J* = 2.4, 9.1 Hz, 1H), 9.64 (s, 1H). LCMS *m/z* = 425.4 [M + H]⁺.

4-Fluoro-*N*-[3-(2-methyl-2*H*-pyrazol-3-yl)-4-(2-morpholin-4-yl-ethoxy)-phenyl]-benzamide (10f). 10f was prepared in a manner similar to that described for 10a, using 9d (60 mg, 0.20 mmol) and 4-fluorobenzoic acid (36 mg, 0.26 mmol) to give the TFA salt of 10f as a white solid (22 mg, 26%). ¹H NMR (DMSO-*d*₆, 400 MHz) δ: 3.02 (m, 2H), 3.14–3.17 (m, 2H), 3.50–3.59 (m, 4H), 3.69 (s, 3H), 3.82–3.85 (m, 2H), 4.36 (t, *J* = 4.8 Hz, 2H), 6.29 (s, 1H), 7.24 (d, *J* = 9.1 Hz, 1H), 7.37 (t, *J* = 8.8 Hz, 2H), 7.49 (s, 1H), 7.72 (s, 1H), 7.88 (dd, *J* = 2.8, 9.1 Hz, 1H), 8.03 (dd, *J* = 5.6, 8.8 Hz, 2H), 9.86 (s, 1H), 10.3 (s, 1H). LCMS *m/z* = 425.4 [M + H]⁺.

***N*-[3-(4-Chloro-2-methyl-2*H*-pyrazol-3-yl)-4-(2-morpholin-4-yl-ethoxy)-phenyl]-3-fluoro-benzamide (10g).** 10g was prepared in a manner similar to that described for 10c and was obtained as the TFA salt as an off-white solid (44%). ¹H NMR (DMSO-*d*₆, 400 MHz) δ: 3.10 (m, 4H), 3.59 (m, 4H), 3.67 (s, 3H), 3.87 (m, 2H), 4.34 (m, 1H), 7.31 (d, *J* = 9.1 Hz, 1H), 7.46 (dt, *J* = 2.5, 9.0 Hz, 1H), 7.59 (m, 1H), 7.67 (s, 1H), 7.73 (d, *J* = 2.6 Hz, 1H), 7.77 (m, 1H), 7.82 (m, 1H), 7.96 (dd, *J* = 2.6, 9.0 Hz, 1H), 10.3 (s, 1H). LCMS *m/z* = 459/461 [M + H]⁺.

***N*-[3-(2-Methyl-2*H*-pyrazol-3-yl)-4-(2-morpholin-4-yl-ethoxy)-phenyl]-4-trifluoromethyl-benzamide (10h).** 10h was prepared in a manner similar to that described for 10a, using 9d (60 mg, 0.20 mmol) and 4-trifluoromethylbenzoic acid (49 mg, 0.26 mmol) to give the TFA salt of 10h as a white solid (27 mg, 28%). ¹H NMR (DMSO-*d*₆, 400 MHz) δ: 3.00–3.03 (m, 2H), 3.16–3.19 (m, 2H), 3.52–3.60 (m, 4H), 3.70 (s, 3H), 3.84–3.87 (m, 2H), 4.39 (t, *J* = 5.0 Hz, 2H), 6.31 (s, 1H), 7.28 (d, *J* = 9.0 Hz, 1H), 7.51 (s, 1H), 7.75 (s, 1H), 7.94 (d, *J* = 8.3 Hz, 2H), 8.16 (d, *J* = 8.8 Hz, 2H), 8.89 (s, 1H), 9.88 (s, 1H), 10.5 (s, 1H). LCMS *m/z* = 475.4 [M + H]⁺.

***N*-[3-(2-Methyl-2*H*-pyrazol-3-yl)-4-(2-morpholin-4-yl-ethoxy)-phenyl]-3-trifluoromethyl-benzamide (10i).** 10i was prepared in a manner similar to that described for 10c, using 9d (50 mg, 0.16 mmol) and 3-trifluoromethylbenzoyl chloride and was obtained as a white solid (72 mg, 92%). ¹H NMR (DMSO-*d*₆, 400 MHz) δ: 2.34 (t, *J* = 4.0 Hz, 4H), 2.61 (t, *J* = 8.0 Hz, 2H), 3.51 (t, *J* = 4.0 Hz, 4H), 3.71 (s, 3H), 4.12 (t, *J* = 8.0 Hz, 2H), 6.26 (d, *J* = 1.8 Hz, 1H), 7.21 (d, *J* = 9.0 Hz, 1H), 7.45 (d, *J* = 1.8 Hz, 1H), 7.69 (d, *J* = 2.6 Hz, 1H), 7.81–7.77 (m, 1H), 7.85–7.82 (m, 1H), 7.97 (d, *J* = 7.8 Hz, 1H), 8.26 (d, *J* = 7.9 Hz, 1H), 8.29 (s, 1H), 10.4 (bs, 1H). LCMS *m/z* = 475 [M + H]⁺.

3,4-Difluoro-*N*-[3-(2-methyl-2*H*-pyrazol-3-yl)-4-(2-morpholin-4-yl-ethoxy)-phenyl]-benzamide (10j). 10j was prepared in a manner similar to that described for 10c, using 9d (120 mg, 0.40 mmol) and 3,4-difluorobenzoyl chloride (84 mg, 0.48 mmol) to give the TFA salt of 10j as a white solid (110 mg, 63%). ¹H NMR (acetone-*d*₆, 400 MHz) δ: 3.11 (bs, 2H), 3.37 (s, 2H), 3.68 (t, *J* = 4.8 Hz, 2H), 3.75 (s, 3H), 3.86 (bs, 4H), 4.59 (t, *J* = 4.8 Hz, 2H), 6.30 (s, 1H), 7.23 (d, *J* = 8.8 Hz, 1H), 7.48 (m, 2H), 7.80 (s, 1H), 7.87–7.92 (m, 2H), 7.93–7.99 (m, 1H), 9.67 (s, 1H). LCMS *m/z* = 443.3 [M + H]⁺.

3-Methoxy-*N*-[3-(2-methyl-2*H*-pyrazol-3-yl)-4-(2-morpholin-4-yl-ethoxy)-phenyl]-benzamide (10k). 10k was prepared in a manner similar to that described for 10c, using 9d (120 mg, 0.40 mmol) and 3-methoxybenzoyl chloride (81 mg, 0.48 mmol) to give the TFA salt of 10k as a white solid (88 mg, 51%); mp (HCl salt, recrystallized from iPrOH) 214–216 °C. ¹H NMR (acetone-*d*₆, 400 MHz) δ: 2.99–3.21 (m, 2H), 3.22–3.45 (m, 2H), 3.66 (t, *J* = 4.8 Hz, 2H), 3.75 (s, 3H), 3.85 (s, 3H), 3.79–3.89 (m, 4H), 4.58 (t, *J* = 4.8 Hz, 2H), 6.29 (d, *J* = 2.0 Hz, 1H), 7.13 (dd, *J* = 2.5, 8.3 Hz, 1H), 7.22 (d, *J* = 8.8 Hz, 1H), 7.42 (t, *J* = 7.8 Hz, 1H), 7.47 (d, *J* = 1.7 Hz, 1H), 7.52 (t, *J* = 1.7 Hz, 1H), 7.56 (d, *J* = 7.0 Hz, 1H), 7.80–7.83 (m, 1H), 7.91–7.96 (m, 1H), 9.54 (s, 1H). LCMS *m/z* = 437.5 [M + H]⁺.

***N*-[3-(2-Methyl-2*H*-pyrazol-3-yl)-4-[2-(3-oxo-piperazin-1-yl)-ethoxy]-phenyl]-3-trifluoromethyl-benzamide (10l).** 10l was prepared in a manner similar to that described for 10c, using 9l (79 mg, 0.25 mmol) and 3-trifluoromethyl benzoyl chloride (63 mg, 0.30 mmol) to give the TFA salt of 10l as a white solid

(52 mg, 41%). ¹H NMR (CD₃CN, 400 MHz) δ: 3.16–3.21 (m, 2H), 3.30–3.36 (m, 2H), 3.48 (t, *J* = 4.8 Hz, 2H), 3.65 (s, 2H), 3.73 (s, 3H), 4.40 (t, *J* = 4.4 Hz, 2H), 6.33 (d, *J* = 1.8 Hz, 1H), 6.65 (s, 1H), 7.14 (d, *J* = 9.0 Hz, 1H), 7.51 (d, *J* = 1.7 Hz, 1H), 7.65 (d, *J* = 2.6 Hz, 1H), 7.72 (t, *J* = 7.8 Hz, 1H), 7.81 (dd, *J* = 2.6, 8.8 Hz, 1H), 7.89 (d, *J* = 7.8 Hz, 1H), 8.18 (d, *J* = 7.8 Hz, 1H), 8.23 (s, 1H), 8.93 (s, 1H). LCMS *m/z* = 488.2 [M + H]⁺.

***N*-[3-(4-Chloro-2-methyl-2*H*-pyrazol-3-yl)-4-[2-(3-oxo-piperazin-1-yl)-ethoxy]-phenyl]-3-trifluoromethyl-benzamide (10m).** 10m was prepared in a manner similar to that described for 10c, using 4-[2-(4-amino-2-(4-chloro-1-methyl-1*H*-pyrazol-5-yl)phenoxy)-ethyl]piperazin-2-one (88 mg, 0.25 mmol) and 3-trifluoromethyl benzoyl chloride (52 mg, 0.25 mmol) to give the TFA salt of 10m as a white solid (70 mg, 53%). ¹H NMR (DMSO-*d*₆, 400 MHz) δ: 3.20–3.24 (m, 4H), 3.62–3.78 (m, 8H), 4.31–4.38 (m, 2H), 7.31 (d, *J* = 9.1 Hz, 1H), 7.65 (s, 1H), 7.71 (d, *J* = 2.8 Hz, 1H), 7.77–7.81 (m, 1H), 7.93–7.99 (m, 2H), 8.25–8.29 (m, 2H), 10.5 (s, 1H). LCMS *m/z* = 522.3/524.2 [M + H]⁺.

***N*-[4-[2-(4-Acetylpiperazin-1-yl)ethoxy]-3-(1-methyl-1*H*-pyrazol-5-yl)phenyl]-3-(trifluoromethyl)benzamide (10n).** 10n was prepared in a manner similar to that described for 10c, using 9n (60 mg, 0.18 mmol) and 3-trifluoromethylbenzoyl chloride (36 mg, 0.18 mmol) to give the TFA salt of 10n as a white solid (36 mg, 40%, 92% purity by LCMS). ¹H NMR (CD₃CN, 400 MHz) δ: 1.94 (s, 3H), 3.32 (t, *J* = 4.8 Hz, 2H), 3.50–3.85 (m, 8H), 3.62 (s, 3H), 4.29 (t, *J* = 4.8 Hz, 2H), 6.23 (s, 1H), 7.03 (d, *J* = 9.1 Hz, 1H), 7.43 (d, *J* = 1.8 Hz, 1H), 7.55–7.82 (m, 4H), 8.08–8.10 (m, 1H), 8.15 (s, 1H), 8.86 (s, 1H). LCMS *m/z* = 516.4 [M + H]⁺.

***N*-[4-[2-(4-Acetylpiperazin-1-yl)ethoxy]-3-(1-methyl-1*H*-pyrazol-5-yl)phenyl]-3-fluorobenzamide (10o).** 10o was prepared in a manner similar to that described for 10c, using 9n (100 mg, 0.29 mmol) and 3-fluorobenzoyl chloride (46 mg, 0.29 mmol) to give the TFA salt of 10o as a white solid (38 mg, 28%); mp (free base, recrystallized from iPrOH/heptane = 70/30) 139–140 °C. ¹H NMR (CD₃CN, 400 MHz) δ: 2.09 (s, 3H), 3.32–3.38 (m, 6H), 3.48 (t, *J* = 4.8 Hz, 4H), 3.79 (s, 3H), 4.43 (t, *J* = 4.8 Hz, 2H), 6.39 (d, *J* = 2.0 Hz, 1H), 7.18 (d, *J* = 9.1 Hz, 1H), 7.40 (dt, *J* = 7.4, 8.6 Hz, 1H), 7.57–7.63 (m, 2H), 7.70–7.74 (m, 2H), 7.80–7.82 (m, 1H), 7.85 (dd, *J* = 2.8, 9.1 Hz, 1H), 8.93 (s, 1H). LCMS *m/z* = 466.4 [M + H]⁺.

***N*-[4-[2-(4-Acetylpiperazin-1-yl)ethoxy]-3-(4-chloro-1-methyl-1*H*-pyrazol-5-yl)phenyl]-3-fluorobenzamide (10p).** 10p was prepared in a manner similar to that described for 10c, using 1-[4-[2-(4-amino-2-(4-chloro-1-methyl-1*H*-pyrazol-5-yl)phenoxy)-ethyl]piperazin-1-yl]ethanone (86 mg, 0.23 mmol) and 3-fluorobenzoyl chloride (43 mg, 0.27 mmol) to give the TFA salt of 10p as an off-white solid (33 mg, 29%). ¹H NMR (CD₃CN, 400 MHz) δ: 1.97 (s, 3H), 2.24–2.38 (m, 4H), 2.60–2.69 (m, 2H), 3.17 (d, *J* = 4.8 Hz, 2H), 3.31–3.36 (m, 2H), 3.67 (s, 3H), 4.07–4.13 (m, 2H), 7.25 (d, *J* = 9.0 Hz, 1H), 7.44 (t, *J* = 8.5 Hz, 1H), 7.56–7.62 (m, 1H), 7.63 (s, 1H), 7.71 (d, *J* = 2.5 Hz, 1H), 7.77 (d, *J* = 9.8 Hz, 1H), 7.81 (d, *J* = 8.0 Hz, 1H), 7.90 (dd, *J* = 9.0, 2.5 Hz, 1H), 10.3 (s, 1H). LCMS *m/z* = 500.7 [M + H]⁺.

***N*-[4-[2-(4-Acetylpiperazin-1-yl)ethoxy]-3-(1-methyl-1*H*-pyrazol-5-yl)phenyl]-3-methoxybenzamide (10q).** Step 1: Preparation of 4-[2-(4-bromo-ethoxy)-3-(2-methyl-2*H*-pyrazol-3-yl)-phenyl]amine. To a solution of *N*-[4-(2-bromo-ethoxy)-3-(2-methyl-2*H*-pyrazol-3-yl)-phenyl]-acetamide (3 g, 8.9 mmol) in methanol (6 mL) at 0 °C was added sulfuric acid (2.2 mL, 42 mmol). The reaction mixture was then heated to reflux for 1.5 h. The mixture was cooled, quenched with water, and cautiously neutralized with sodium hydroxide solution until the pH was around 7. The mixture was extracted twice with ethyl acetate, and the combined organic layers concentrated in vacuo to give the title compound as an off-white solid (2.6 g, 99%). LCMS *m/z* = 296.1/298.1 [M + H]⁺. The intermediate was used in the next step without further purification.

Step 2: Preparation of *N*-[4-(2-Bromo-ethoxy)-3-(2-methyl-2*H*-pyrazol-3-yl)-phenyl]-3-methoxy-benzamide. A mixture of the intermediate obtained from step 1 (1.01 g, 3.42 mmol),

3-methoxy-benzoyl chloride (700 mg, 4.10 mmol), and triethylamine (1.0 mL) in THF (5 mL) was stirred at room temperature for 10 min. Excess solvent was evaporated and the crude product redissolved in acetonitrile. H₂O was added slowly to eventually provide an approximately 3/2 CH₃CN/H₂O v/v mixture, and the resulting precipitate was collected by filtration and dried to give the title compound as an off-white solid (957 mg, 65%). LCMS *m/z* = 430.3/432.3 [M + H]⁺. This was used in the next step without further purification.

Step 3: Preparation of *N*-{4-[2-(4-Acetylpiperazin-1-yl)ethoxy]-3-(1-methyl-1*H*-pyrazol-5-yl)phenyl}-3-methoxybenzamide (10q). A mixture of the intermediate obtained from step 2 (90 mg, 0.21 mmol), 1-piperazin-1-yl-ethanone (32 mg, 0.25 mmol), and K₂CO₃ (116 mg, 0.84 mmol) in DMF (2 mL) was heated under microwave irradiation at 120 °C for 20 min. The crude reaction mixture was purified by HPLC to give the TFA salt of **10q** as a white solid (97 mg, 97%). ¹H NMR (acetone-*d*₆, 400 MHz) δ: 2.07 (s, 3H), 3.30 (bs, 4H), 3.71 (t, *J* = 4.8 Hz, 2H), 3.75 (s, 3H), 3.79 (bs, 2H), 3.87 (s, 3H), 4.60 (t, *J* = 4.8 Hz, 2H), 4.99 (bs, 2H), 6.32 (s, 1H), 7.13 (d, *J* = 8.0 Hz, 1H), 7.23 (d, *J* = 9.0 Hz, 1H), 7.42 (t, *J* = 8.0 Hz, 1H), 7.53 (m, 2H), 7.56 (d, *J* = 7.8 Hz, 1H), 7.82 (s, 1H), 7.94 (dd, *J* = 8.8, 2.5 Hz, 1H), 9.56 (s, 1H). LCMS *m/z* = 478.3 [M + H]⁺.

4-[2-[4-(3-Methoxy-benzoylamino)-2-(2-methyl-2*H*-pyrazol-3-yl)-phenoxy]-ethyl]-piperazine-1-carboxylic Acid Amide (10r). **10r** was prepared in a manner similar to that described for **10q**, using the intermediate from step 2 of **10q** (90 mg, 0.21 mmol) and piperazine-1-carboxamide (32 mg, 0.25 mmol) to give the TFA salt of **10r** as a white solid (52 mg, 52%). ¹H NMR (CD₃CN, 400 MHz) δ: 2.70–3.25 (m, 6H), 3.30–3.37 (m, 1H), 3.40 (t, *J* = 4.8 Hz, 2H), 3.71 (s, 3H), 3.86 (s, 3H), 4.36 (t, *J* = 4.8 Hz, 2H), 5.13 (bs, 2H), 6.30 (s, 1H), 7.11 (d, *J* = 9.0 Hz, 1H), 7.14 (d, *J* = 8.0 Hz, 1H), 7.43 (t, *J* = 7.8 Hz, 1H), 7.45 (s, 1H), 7.49 (d, *J* = 7.8 Hz, 1H), 7.51 (s, 1H), 7.63 (s, 1H), 7.80 (d, *J* = 9.0 Hz, 1H), 8.75 (s, 1H). LCMS *m/z* = 479.4 [M + H]⁺.

3-Methoxy-*N*-{3-(1-methyl-1*H*-pyrazol-5-yl)-4-[2-(4-(methylsulfonyl)piperazin-1-yl)ethoxy]phenyl}benzamide (10s). **10s** was prepared in a manner similar to that described for **10q**, using the intermediate from step 2 of **10q** (90 mg, 0.21 mmol) and 1-(methylsulfonyl)-piperazine (41 mg, 0.25 mmol) to give the TFA salt of **10s** as a white solid (65 mg, 61%). ¹H NMR (CD₃CN, 400 MHz) δ: 2.85 (s, 3H), 3.05–3.67 (m, 8H), 3.44 (t, *J* = 4.7 Hz, 2H), 3.72 (s, 3H), 3.86 (s, 3H), 4.37 (t, *J* = 4.7 Hz, 2H), 6.32 (d, *J* = 1.8 Hz, 1H), 7.10–7.16 (m, 2H), 7.41–7.55 (m, 4H), 7.65 (d, *J* = 2.4 Hz, 1H), 7.82 (dd, *J* = 8.8, 2.5 Hz, 1H), 8.76 (s, 1H). LCMS *m/z* = 514.5 [M + H]⁺.

***N*-{4-[2-(2-Hydroxyethylamino)ethoxy]-3-(1-methyl-1*H*-pyrazol-5-yl)phenyl}-3-methoxybenzamide (10t).** **10t** was prepared in a manner similar to that described for **10q**, using the intermediate from step 2 of **10q** (200 mg, 0.46 mmol) and ethanolamine (43 mg, 0.70 mmol) to give the TFA salt of **10t** as a white solid (150 mg, 78%). ¹H NMR (DMSO-*d*₆, 400 MHz) δ: 2.82–2.90 (m, 2H), 3.30–3.36 (m, 2H), 3.50–3.55 (m, 2H), 3.69 (s, 3H), 3.83 (s, 3H), 4.24–4.28 (m, 2H), 6.32 (d, *J* = 1.8 Hz, 1H), 7.14–7.18 (m, 1H), 7.21 (d, *J* = 9.1 Hz, 1H), 7.42–7.55 (m, 4H), 7.61 (d, *J* = 2.4 Hz, 1H), 7.88 (dd, *J* = 9.0, 2.5 Hz, 1H), 7.89–7.95 (br s, 2H), 10.2 (s, 1H). LCMS *m/z* = 411.4 [M + H]⁺.

***N*-[4-(2-Aminoethoxy)-3-(1-methyl-1*H*-pyrazol-5-yl)phenyl]-3-methoxybenzamide (10u).** **10u** was prepared in a manner similar to that described for **10q**, using the intermediate from step 2 of **10q** (500 mg, 1.16 mmol) and ammonia in methanol (11.6 mmol) to give the TFA salt of **10u** as a white solid (226 mg, 53%). ¹H NMR (DMSO-*d*₆, 400 MHz) δ: 3.11–3.22 (m, 2H), 3.71 (s, 3H), 3.85 (s, 3H), 4.16 (t, *J* = 5.8 Hz, 2H), 6.36 (d, *J* = 1.8 Hz, 1H), 7.14–7.18 (m, 1H), 7.24 (d, *J* = 9.0 Hz, 1H), 7.42–7.55 (m, 4H), 7.65 (d, *J* = 2.4 Hz, 1H), 7.82 (dd, *J* = 9.0, 2.5 Hz, 1H), 7.89–7.95 (br s, 3H), 10.2 (s, 1H). LCMS *m/z* = 367.5 [M + H]⁺.

Biological Assays. [¹²⁵I]DOI Binding to Recombinant Human 5-HT_{2A} and 5-HT_{2C} Receptors. Radioligand binding assays for

human 5-HT_{2A} and 5-HT_{2C} receptors were developed using crude plasma membranes prepared from HEK293 cells stably expressing these receptors.²¹ The 5-HT₂ agonist [¹²⁵I]DOI (0.5 nM) was used as radioligand and nonspecific radioligand binding was determined in the presence of 10 μM cold DOI. Competition experiments consisted of addition of 95 μL of assay buffer (20 mM HEPES, pH 7.4, 10 mM MgCl₂), 50 μL of membranes (5–25 μg protein), 50 μL of [¹²⁵I]DOI (0.5 nM final assay concentration), and 5 μL of test compound diluted in assay buffer (final concentrations ranging from 1 pM to 10 μM) to 96-well Perkin-Elmer GF/C microtiter plates, and incubations were performed for one hour at room temperature. Each radioligand competition study consisted of testing eight different concentrations in which triplicate determinations were performed for each test compound concentration. Assay incubations were terminated by rapid filtration of microtiter plates under vacuum pressure using a Brandell cell harvester, followed by washing filter plates several times with ice-cold wash buffer (50 mM Tris-HCl, pH 7.4). Plates were then dried at 45 °C in an oven for a minimum of two hours, 25 μL of BetaScint scintillation cocktail was added to each well, and microtiter plates were counted in a Packard TopCount scintillation counter.

Human Platelet Aggregation Assay. Platelet aggregation was measured turbidometrically at 37 °C. Platelet rich plasma was prepared from anticoagulated whole blood obtained from male and female donors. Platelet concentrations in the platelet rich plasma were adjusted to 250,000 platelets/μL using platelet poor plasma, then 500 μL of platelet rich plasma was preincubated at 37 °C and stirred at 1200 rpm with inhibitors for 1 min before induction of aggregation by the simultaneous addition of 5-HT (final concentration 1 μM) and ADP (final concentration 1 μM). The maximal amplitude of aggregation response within 3 min was measured in triplicate using the Chronolog model 490 aggregometer. Percent inhibition of aggregation was calculated from the maximum decrease in optical density of the controls and of the samples containing inhibitor.

Rat Pharmacokinetics. Male Sprague–Dawley rats were dosed orally or intravenously at 10 and 2 mg/kg, respectively, in 80% PEG400 and 20% phosphate buffered saline. Animals were fasted overnight prior to oral dose administration. Whole blood samples were collected from the jugular vein over a 24 h period postdose. Plasma was prepared from sodium heparin treated whole blood and separated by centrifugation. Plasma samples were assayed using a selective HPLC/MS/MS method. The HPLC/MS/MS was operated in multiple reaction monitoring (MRM) mode under optimized conditions for detection of selected compounds and the internal standard using positive ions formed by electrospray ionization. Quantitation was determined using a weighted regression analysis of peak area ratios of analyte and internal standard. The method provided a lower limit of quantitation of 1 ng/mL and an upper limit of quantitation of 2000 ng/mL. Serial sampling (at 0.25, 0.5, 1, 2, 4, 6, 8, 10, 12, 15, 18 and 21 h post dosing) was used to define the plasma concentration vs time profile.

Acknowledgment. We thank Juan Ramirez, Chen Liaw, William J. Thomsen, and Joel Gatlin for additional technical support.

References

- (1) (a) Chackalamannil, S. Thrombin receptor (protease activated receptor-1) antagonists as potent antithrombotic agents with strong antiplatelet effects. *J. Med. Chem.* **2006**, *49*, 5389–5403. (b) Chackalamannil, S.; Wang, Y.; Greenlee, W. J.; Hu, Z.; Xia, Y.; Ahn, H.; Boykow, G.; Hsieh, Y.; Palamanda, J.; Agans-Fantuzzi, J.; Kurowski, S.; Graziano, M.; Chintala, M. Discovery of a novel, orally active himbacine-based thrombin receptor antagonist (SCH 530348) with potent antiplatelet activity. *J. Med. Chem.* **2008**, *51*, 3061–3064. (c) Becker, R. C.; Moliterno, D. J.; Jennings, L. K.; Pieper, K. S.; Pei, J.; Niederman, A.; Ziada, K. M.; Berman, G.; Strony, J.; Joseph, D.;

- Mahaffey, K. W.; Van De Werf, F.; Veltri, E.; Harrington, R. A. Safety and tolerability of SCH 530348 in patients undergoing nonurgent percutaneous coronary intervention: a randomized, double-blind, placebo-controlled phase II study. *The Lancet* **2009**, 373, 919–928.
- (2) Hoyer, D.; Hannon, J. P.; Martin, G. R. Molecular, pharmacological and functional diversity of 5-HT receptors. *Pharmacol., Biochem. Behav.* **2002**, 71, 533–554.
- (3) Doyle, A. E. Serotonin antagonists and vascular protection. *Cardiovasc. Drugs Ther.* **1990**, 4, 13–18.
- (4) Nagatomo, T.; Rashid, M.; Abul Muntasir, H.; Komiyama, T. Functions of 5-HT_{2A} receptor and its antagonists in the cardiovascular system. *Pharmacol. Ther.* **2004**, 104, 59–81.
- (5) De Clerk, F. F.; Herman, A. G. 5-Hydroxytryptamine and platelet aggregation. *Fed. Proc.* **1983**, 42, 228–232.
- (6) De Clerk, F. F.; Janssen, P. A. Amplification mechanisms in platelet activation and arterial thrombosis. *J. Hypertens. Suppl.* **1990**, 8, S87–S93.
- (7) Klein, W.; Eber, B.; Dusleag, J.; Rotman, B.; Koltringer, P.; Luka, O.; Vanhoutte, P. M. Ketanserin prevents early restenosis following percutaneous transluminal coronary angioplasty. *Clin. Physiol. Biochem.* **1990**, 8 (Suppl. 3), 101–107.
- (8) Kyriakides, Z. S.; Sbarouni, E.; Nikolaou, N.; Antoniadis, A.; Kremastinos, D. T. Intracoronary ketanserin augments coronary collateral blood and decreases myocardial ischemia during balloon angioplasty. *Cardiovasc. Drugs Ther.* **1999**, 13, 415–422.
- (9) Serruys, P. W.; Klein, W.; Tijssen, J. P.; Rutsch, W.; Heyndrickx, G. R.; Emanuelsson, H.; Ball, S. G.; Decoster, O.; Schroeder, E.; Liberman, H. Evaluation of ketanserin in the prevention of restenosis after percutaneous transluminal coronary angioplasty. A multicenter randomized double-blind placebo-controlled trial. *Circulation* **1993**, 88, 1588–1601.
- (10) Fujita, M.; Mizuno, K.; Ho, M.; Tsukahara, R.; Miyamoto, A.; Miki, O.; Ishii, K.; Miwa, K. Sarpogrelate treatment reduces restenosis after coronary stenting. *Am. Heart J.* **2003**, 145 (3), E16.
- (11) Teegarden, B.; Jayakumar, H.; Li, H.; Strah-Pleynt, S.; Dosa, P. I. Diaryl and arylheteroaryl urea derivatives as modulators of the 5-HT_{2A} serotonin receptor useful for the prophylaxis and treatment of disorders related thereto. Patent PCT/US2004/023488, WO2005012254, Feb 10, **2005**.
- (12) Teegarden, B. R.; Li, H.; Jayakumar, H.; Strah-Pleynt, S.; Dosa, P. I.; Selaya, S. D.; Kato, N.; Elwell, K. H.; Davidson, J.; Cheng, K.; Saldana, H.; Frazer, J. M.; Whelan, K.; Foster, J.; Espitia, S.; Webb, R. R.; Beeley, N. R. A.; Thomsen, W.; Morairty, S. R.; Kilduff, T. S.; Al-Shamma, H. A. Discovery of 1-[3-(4-Bromo-2-methyl-2H-pyrazol-3-yl)-4-methoxy-phenyl]-3-(2,4-difluoro-phenyl)-urea (Nelotanserin) and related 5-hydroxytryptamine_{2A} inverse agonists for the treatment of insomnia. *J. Med. Chem.* **2010**, 53, 1923–1936.
- (13) Teegarden, B.; Xiong, Y.; Strah-Pleynt, S.; Jayakumar, H.; Dosa, P. I.; Feichtinger, K.; Casper, M.; Lehmann, J.; Jones, R. M.; Unett, D. J. 3-Phenyl-pyrazole derivatives as modulators of the 5-HT_{2A} serotonin receptor useful for the treatment of disorders related thereto. Patent PCT/US2005/041726, WO2006055734, May 26, **2006**.
- (14) Dosa, P. I.; Strah-Pleynt, S.; Jayakumar, H.; Casper, M.; Decaire, M.; Xiong, Y.; Lehmann, J.; Choi, K.; Elwell, K.; Wong, A.; Webb, W.; Adams, J. W.; Ramirez, J.; Richman, J. G.; Thomsen, W.; Semple, G.; Teegarden, B. R. *Bioorg. Med. Chem. Lett.* **2009**, 19, 5486–5489.
- (15) Adams, J. W.; Ramirez, J.; Ortuno, D.; Shi, Y.; Thomsen, W.; Richman, J. G.; Morgan, M.; Dosa, P.; Teegarden, B. R.; Al-Shamma, H.; Behan, D. P.; Connolly, D. T. Anti-thrombotic and vascular effects of AR246686, a novel 5-HT_{2A} receptor antagonist. *Eur. J. Pharmacol.* **2008**, 586, 234–243.
- (16) Jamieson, C.; Moir, E. M.; Rankovic, Z.; Wishart, G. Medicinal chemistry of hERG optimization: highlights and hang-ups. *J. Med. Chem.* **2006**, 49, 5029–5046.
- (17) Aronov, A. M. Common pharmacophores for uncharged human ether-a-go-go-related gene (hERG) blockers. *J. Med. Chem.* **2006**, 49, 6917–6921.
- (18) pK_a values were calculated using ACDLABS 12.0 pK_a dB, and the values were reported as the highest basic pK_a.
- (19) For details of APD791 and its active metabolites pharmacokinetics and pharmacology, see: Adams, J. W.; Ramirez, J.; Shi, Y.; Thomsen, W.; Frazer, J.; Morgan, M.; Edwards, J. E.; Chen, W.; Teegarden, B. R.; Xiong, Y.; Al-Shamma, H.; Behan, D. P.; Connolly, D. T. APD791, a novel 5-hydroxytryptamine 2A receptor antagonist: pharmacological profile, pharmacokinetics, platelet and vascular biology. *J. Pharmacol. Exp. Ther.* **2009**, 331, 96–103.
- (20) Przyklenk, K.; Frelinger, A. L., III; Linden, M. D. Whittaker, P.; Li, Y.; Barnard, M. R.; Adams, J.; Morgan, M.; Al-Shamma, H.; Michelson, A. D. Targeted inhibition of the serotonin 5HT-(2A) receptor improves coronary patency in an in vivo model of recurrent thrombosis. *J. Thromb. Haemostasis* **2009**, 8, 331–340.
- (21) Thomsen, W. J.; Grottick, A. J.; Menzaghi, F.; Reyes-Saldana, H.; Espitia, S.; Yuskin, D.; Whelan, K.; Martin, M.; Morgan, M.; Chen, W.; Al-Shamma, H.; Smith, B.; Chalmers, D.; Behan, D. Lorcaserin, a novel selective human 5-hydroxytryptamine_{2C} agonist: in vitro and in vivo pharmacological characterization. *J. Pharmacol. Exp. Ther.* **2008**, 325 (2), 577–587.
- (22) Cheng, Y. C.; Prusoff, W. H. Relationship between the inhibition constant (K_i) and the concentration which causes 50% inhibition (IC₅₀) of an enzymatic reaction. *Biochem. Pharmacol.* **1973**, 22, 3099–3108.